

ROYAL  
DEFENCE



PROCUREMENT EXECUTIVE, MINISTRY OF DEFENCE

AERONAUTICAL RESEARCH COUNCIL  
REPORTS AND MEMORANDA

# A New Probe for the Direct Measurement of Stagnation Pressure in Supersonic Flow

By M. J. GOODYER  
The University, Southampton

LONDON: HER MAJESTY'S STATIONERY OFFICE

1975

PRICE £1.66 NET

# A New Probe for the Direct Measurement of Stagnation Pressure in Supersonic Flow

By M. J. GOODYER  
The University, Southampton

---

*Reports and Memoranda No. 3762\**  
*December, 1973*

---

## Summary

The probe decelerates a portion of the supersonic free stream into the subsonic range within a distributed compression fan. Stagnation pressure is sampled in the region of subsonic flow using a pitot tube. Pressure recovery has been measured over the Mach number range 1.5 to 2.5, a typical value being 0.999 at a Mach number of 1.88. The probe is usefully insensitive to misalignment with the free stream and pressure tappings in the compression surface allow it to be used also as a flow-direction sensor.

---

\* Replaces R.A.E. Technical Report 73122—A.R.C. 35 388.

## LIST OF CONTENTS

1. Introduction
  2. Background
  3. Description of the Probe
  4. Test Apparatus
  5. The Flow Field Generated by the Probe
  6. Conditions on the Attachment Line
  7. Measurements of Pressure Recovery
  8. Flow Direction Sensing
    - 8.1. Pitch sensing
    - 8.2. Yaw sensing
  9. Flow Deflection for Sonic Flow
  10. Conclusions
- Acknowledgments
- List of Symbols
- References
- Appendix A
- Appendix B
- Tables 1 to 5
- Illustrations Figs. 1 to 15
- Detachable Abstract Cards

## 1. Introduction

A new probe sensor has been developed which can measure the full stagnation pressure in supersonic flow, a property which hitherto could only be estimated indirectly from other measurements. The probe has been tested in a supersonic wind-tunnel in the Mach number range from 1.5 to 2.5 at the Royal Aircraft Establishment, Farnborough.

The motivation for the development of the probe may be illustrated by the following two examples.

### (i) *In-flight thrust estimation*

In order to correlate full-scale aircraft drag with wind-tunnel model measurements, engine thrust and hence aircraft drag are sometimes estimated from pressure-probe measurements in the exhaust. The equation for thrust per unit area is

$$T = P \left\{ \frac{2\gamma}{\gamma - 1} \left[ \left( \frac{P_t}{P} \right)^{(\gamma-1)/\gamma} - 1 \right] + 1 \right\} - P_\alpha$$

where  $P_t$  = stream stagnation pressure,

$P$  = stream static pressure,

$P_\alpha$  = ambient static pressure

and  $\gamma$  = ratio of specific heats.

The normal method of measurement is to swing a pitot- and static-probe rake across the exhaust to allow integration of the above equation. In supersonic flow the measured pitot pressure requires correcting by a factor  $F$  to convert it to the stagnation pressure  $P_t$ . The factor  $F$  is a function of Mach number and the ratio of specific heats and is plotted on Fig. 1. The particular problem of estimating this factor has been identified<sup>1</sup> as a major source of error in the estimation of in-flight thrust from the measurements of conventional probes.

As an alternate sensor to the pitot tube, the wedge probe can be considered. The wedge generates a partially decelerated flow field downstream of an oblique shock in which the local flow is usually still supersonic, where a pitot tube samples the local pitot pressure. Over most of the supersonic Mach number range this probe registers a pressure which is closer to stagnation pressure than that registered by an isolated pitot tube, and hence a smaller correction applies. It might be expected that the sensitivity of the magnitude of the correction to uncertainties in the local Mach number or gas properties would also be lower. However, the use of this probe in flows which contain wide variations of Mach number would introduce another difficulty. In the low supersonic range the pressure registered by the wedge probe can become uncertain when the shock is detached from the wedge leading edge. In this Mach number range, which might extend from 1.0 to 1.6 depending on geometry, the probe would need calibrating over a range of  $M_0$  and  $\gamma$  to be of use. With either of these probes, the conventional pitot tube or the wedge probe, errors in the estimation of  $M_0$  or  $\gamma$  introduce errors into the estimation of stagnation pressure from the probe pressure, which increase rapidly with free-stream Mach number as shown in Fig. 1.

### (ii) *The estimation of Mach number*

Baron has shown<sup>2</sup> that the most accurate estimation of Mach number from probe measurements in supersonic flow would be obtained if one of the probes could be arranged to measure stagnation pressure. Baron shows, for example, that at a free-stream Mach number  $M_0 = 2$ , the likely error which would arise from the use of stagnation and static pressures in the computation of  $M_0$  would be about half of the error resulting from the use of pitot and static pressures.

Where Mach number is computed automatically, as for example in an aircraft air-data computer, the measurement of stagnation pressure together with the usual static pressure would simplify computation. When using pressure indications from a conventional pitot static tube, at subsonic flight speeds the computer solves an equation for  $M_0$  in which it is assumed that the pitot tube registers stagnation pressure. In supersonic flight the computer is required to solve a second equation which takes into account the existence of the shock at the pitot tube. With a stagnation pressure probe replacing the pitot tube, the computer would be required to solve only the first of these equations at any flight Mach number.

## 2. Background

The probe which is the subject of this Report was an outcome of some earlier work on an instrument of different geometry.<sup>3</sup> The earlier probe comprised two principal parts, a compression surface which consisted of a long straight circular cylinder, and a pitot tube. The function of the compression surface was similar to that of the above mentioned wedge, namely to generate adjacent to itself a partially decelerated flow field in

which the pitot tube could sample the local pitot pressure. It is necessary for the compression surface to be of such a geometry that any adverse pressure gradients which exist are not sufficient to induce a separation of the boundary layer in a manner which could generate a shock wave anywhere along the streamlines which are sampled by the pitot tube. The straight cylindrical compression surface satisfied this requirement. Nowhere on the leading edge of the cylinder is there an adverse pressure gradient. The relevant flow field ahead of a hypothetical infinitely long cylinder is amenable to exact analysis. Ref. 3 shows that when the cylinder is swept-back relative to the free stream at an angle of about 45 degrees (for  $\gamma = 1.4$  the precise angle is  $\cos^{-1}(1/2.2)^{1/2} \approx 47.61$  degrees) a pitot tube which is arranged to sample the local flow at the attachment line will record full free-stream total (stagnation) pressure at all free-stream Mach numbers up to about 1.5 (for  $\gamma = 1.4$  the exact value of this Mach number is  $(2.2)^{1/2} \approx 1.483$ ). Hence the pressure recovery  $R$ , defined as the ratio of the pressure recorded by the probe to the free-stream total pressure would be unity for this probe over the range of Mach number 0 to about 1.5.

Measurements in a wind tunnel at the Royal Aircraft Establishment, Farnborough, at a Mach number of 1.53 showed that this type of probe would develop a pressure recovery tending to the theoretical value (that theoretically predicted for a probe comprising an infinitely long compression surface) as the length of cylinder increased upstream of the pitot tube. With about 20 cylinder diameters upstream, the pressure recovery reached 0.997. This compared with 0.920 for a pitot tube in air. With increase of length of cylinder upstream of the pitot tube there was also a trend in the flow conditions along the sampled streamline towards those predicted in theory. A pitot tube positioned far from the leading tip of a finite cylinder samples a streamline which has penetrated only a weak bow shock in an otherwise isentropic diffusion process. This is in contrast to the case where a pitot tube is situated near to the leading tip, when the sampled streamline traverses a stronger region of the bow shock. In the case of a pitot at the leading tip, the shock would reach the limit of a normal shock. While the measured pressure recovery is satisfactorily high, with this simple geometry of probe there is no chance of holding a similar level of pressure recovery at higher Mach numbers. For example, at a Mach number of 2.5 the pressure recovery of a 'long' straight cylindrical probe in air would be 0.813, compared with 0.499 for a pitot tube.

An undesirable feature of the above probes was the large size that was required in practice in order to achieve a good pressure recovery. Even when using the rather small outside diameter of pitot tube of  $\frac{1}{2}$  mm the dimensions of the compression surface were diameter 6.35 mm and length 152 mm. These two undesirable features, namely the large size and the 'limiting' Mach number for unity pressure recovery of 1.483 in air prompted a search for an alternate design.

A strongly favourable pressure gradient along the attachment line and extending five or six cylinder diameters downstream from the leading tip of the compression surface had been discovered on these probes. This suggested that the leading section of the cylinder could to some extent be turned into the flow without generating an adverse pressure gradient along the attachment line, and the cylinder would then have taken a shape similar in many respects to the leading edge of a crescent wing. The curved section of the cylinder could apparently extend about six diameters back from the leading tip, judging from the pressure distributions on straight cylinders. By curving the cylinder leading edge into the flow near the leading tip it was reasoned that the strong bow shock would be weakened in the region, to be replaced in part by a distributed zone of deceleration, and as a consequence the shock would everywhere be weakened. The probe could then be made smaller.

A characteristic feature of the flow over the leading-edge region of a swept cylinder is that the boundary layer is rather thin, since it is continuously swept away from the leading edge. The existence of a thin boundary layer suggested that the cylinder leading tip might be curved into the flow even more strongly such that an adverse pressure gradient existed along the attachment line. The notion was that a thin boundary layer might penetrate the pressure gradient without a separation and therefore without the generation of unwanted shocks. The probe would now comprise a curved cylindrical compression surface with a pitot tube sampling the attachment-line flow, the shape also offering the possibility of a more compact design than a straight cylinder. The following sections of this Report describe such a probe.

While a circular cross-section of compression surface has been chosen for the preceding discussion, and for the majority of the probes which have been tested, there may not be a strong case for adhering to that cross-section. For example, a square cross-section might perform well. One such probe has been made and tested at  $M_0 = 2.48$ , where it developed a pressure recovery comparable with the circular-sectioned probes. The design of the probes is the subject of British Patent No. 1308080 (1973), and U.S.A. patent No. 3,832,903 (1974).

### 3. Description of the Probe

The probe comprises two parts, a compression surface and a pitot tube. The compression surface is a cylinder curved along its axis as shown in Fig. 2, and the pitot tube lies adjacent to this surface, facing along the attach-

ment line into the local flow. The dimensions shown in Fig. 2a are nominal only. The profile of the leading edge of the probe tested has been measured and more precise co-ordinates for the curved region are given in Fig. 3. Included in this figure are the locations of four static-pressure tappings on the attachment line also in the curved region of the cylinder.

The compression surface was made from bright mild steel stock with no further machining along the cylindrical surface, and the pitot tube from stainless steel with its opening stoned square with the tube axis. The pitot tube was soldered onto a saddle around the compression surface, the closest point of the saddle being 10.4 mm downstream of the pitot tube opening.

The compression surface was designed to terminate in a fairly long straight cylindrical section swept back at an angle of 35 degrees relative to the free stream. The straight section is a legacy of the background of this probe, and is not required. The essential portion of the compression surface is only the curved part up to the beginning of the straight section as suggested in Fig. 2b.

The attachment line at the tip of the compression surface was arranged to present zero incidence to the free stream, by aligning the tangent to the attachment line parallel to the free stream. In order to leave some strength in the tip, the cylinder was cut off along a line inclined at approximately 7 degrees into the free stream. This left a pronounced 'heel' on the underside of the cylinder.

#### 4. Test Apparatus

The performance of the probe has been evaluated in a supersonic wind tunnel by Aerodynamics Department at R.A.E., Farnborough. Test Mach numbers were 1.53, 1.88 and 2.48. The pressures in the total- and static-pressure lines from the sting-mounted probe were measured on precision Midwood manometers.

The sting could be rotated on a quadrant in one plane while positioning the probe nominally in the centre of the working section. By rolling the probe on the sting both yaw and pitch data were obtained. Pitch is defined as rotation of the probe in the plane of symmetry of the probe, the plane of the sketch on Fig. 2. Yaw is rotation about a vertical axis in this plane.

Free-stream Mach number was determined from measurements of stagnation pressure in the tunnel settling chamber and static pressure at the liner. The frost-point of the air was measured at about  $-40^{\circ}\text{C}$  at the tunnel stagnation pressure of one atmosphere. The effect of any water condensation on the stagnation pressure in the working section is very small at the water concentrations represented by this level of dewpoint. According to predictions<sup>4</sup> a loss of stagnation pressure of about 0.3 per cent could occur with such a frost point, if condensation occurs. It is recognised that moisture condensation could have accounted for some loss of stagnation pressure particularly at  $M_0 = 2.48$ , but in the absence of proper means for checking on the occurrence or effects, the stagnation pressure in the working section was assumed equal to that in the settling chamber. Following this assumption, the pressure recovery  $R$  was defined for the purposes of the tests as the ratio of the pressure recovered by the pitot tube on the probe to the tunnel settling chamber stagnation pressure.

The instrumentation allowed static pressures to be measured to an accuracy of approximately  $\pm 0.1$  per cent. The difference between the probe pitot and the settling chamber total pressure, from which pressure recovery was calculated, was generally rather small and was measured by a differential pressure transducer in order to obtain better resolution. Pressure recovery as here defined could be measured to an accuracy of about  $\pm 0.05$  per cent.

#### 5. The Flow Field Generated by the Probe

Fig. 2b is a sketch of the flow field ahead of the probe. As the flow approaches the compression surface, the free stream is turned in a compression fan sufficient to produce a Mach number somewhat less than unity near to the surface at the downstream end of the curved portion of the cylinder. In this region, the pitot tube samples stagnation pressure. As will be shown later, over a range of free-stream Mach number the compression process undergone by the streamlines which are sampled by the pitot is free from shock and viscous effects, and therefore is isentropic.

The three-dimensional nature of the surface is the feature which prevents the boundary layer from becoming thick over the leading-edge region which is subject to the adverse pressure gradient.

The compression fan converges to coalesce in a shock, but the shock is clear of the streamlines which are sampled by the pitot tube. Early measurements with a traversing pitot tube mounted close to the compression surface indicated that the boundary layer was too thin to significantly affect the pressure recovery with the size of pitot tube shown on Fig. 2, even with the pitot tube adjacent to the surface. Consequently, all subsequent measurements were made with the pitot tube touching the cylinder.

Fig. 4 is a Schlieren picture of the probe under test at  $M_0 = 1.53$ , with zero yaw and a sweepback angle  $\Lambda$  of 35 degrees. The absence of a shock at the pitot tube is some evidence of subsonic flow in that region.

## 6. Conditions on the Attachment Line

The static pressure distribution along the attachment line has been measured at  $M_0 = 1.53$  and 1.88 with the pitot tube removed. Figs. 5 and 6 show the ratio of local static pressure on the attachment line to free-stream stagnation pressure,  $P_a/P_t$ , and also the local Mach number on the attachment line  $M_a$ , as functions of sweepback angle. A progressive increase of pressure with increase of distance from the tip of the compression surface is evident, along the curved portion of the cylinder which extends about 55 mm from the tip.

$M_a$  is seen to progress smoothly to a value of unity or less in the examples shown. There is no evidence of a shock in this region of the flow field.

The influence of sweepback angle is quite strong. With increased sweepback, static pressures fall and Mach numbers increase.

Static pressures are nominally constant (at fixed sweepback and  $M_0$ ) over the straight section of the compression surface. Mach number distributions are not shown for the straight sections, because  $M_a$  is calculated from local stagnation and static pressures, and the local stagnation pressure is not known with certainty beyond the position of the opening of the pitot tube. In regions very far from the tip the static pressure may be calculated exactly according to the theory for infinite straight swept cylinders which is presented in Ref. 3. In Table 1 the measured pressure ratio  $P_a/P_t$  at the tapping farthest from the tip is compared with the infinite cylinder theory.

The measured static pressures shown in Table 1 were taken on the straight section of the compression surface at a position 87 mm from the leading tip measured along the attachment line.

There is fair agreement between theory and practice, with the best agreement at low values of sweepback. It can be seen from the pressure distributions on Figs. 5 and 6 that there is also a tendency for the static pressure to reach its 'straight section' level sooner at low than at high values of sweepback.

## 7. Measurements of Pressure Recovery

Pressure recovery was measured at the three values of free-stream Mach number, and with the geometry of probe shown on Fig. 2. The variation of pressure recovery with sweepback at zero yaw for the lower two values of Mach number is shown on Fig. 7. The peak pressure recovery was 0.999, held constant over a useful range of sweepback angle. Table 2 summarises the pressure recovery data from Fig. 7.

At both values of Mach number the ranges of sweepback shown in the table are centred on a sweepback angle of about 35 degrees. At this value of sweepback the tangent to the attachment line at the leading tip of the compression surface is parallel to the free-stream direction. This was the 'design' attitude of the probe.

Corresponding measurements of the variation of pressure recovery with yaw at a constant sweepback angle  $\Lambda$  of 35 degrees (relative to the support sting) are shown on Fig. 8. Table 3 shows the ranges of yaw where high values of pressure recovery are obtained.

Some asymmetry is apparent on Fig. 8 and in Table 3. Minor inaccuracies in the construction of the probe may have been responsible.

The above evidence suggests that a plateau in the ranges of pitch and yaw exists where pressure recovery is constant and high. The plateau may be elliptical in shape with major and minor axes corresponding to the angles shown in Tables 2 and 3.

For comparison with the maximum pressure recovery of this probe, 0.999 at  $M_0 = 1.53$  and 1.88, it is worth noting that the maximum pressure recovery of a pitot tube at the same Mach numbers in air would be 0.9200 and 0.7765 respectively.

The measurements of pressure recovery at  $M_0 = 2.48$  are shown on Figs. 9 and 10. The maximum pressure recovery is 0.990, achieved at the design sweepback angle of 35 degrees with zero yaw. The loss of stagnation pressure of 1 per cent is significant, and may be explained partly by condensation, as indicated in Section 4. However, further loss probably occurs in one or two shocks lying along the path of the sampled streamline. It is possible that the streamline first penetrates a weak bow shock ahead of the curved part of the compression surface. A second shock probably lies just ahead of the pitot tube because the flow turning of about 48 degrees to the pitot tube is insufficient to decelerate the attachment line flow through the sonic point.

There was some unsteadiness in pressure measurements, both in the static pressures on the attachment line and in the probe pitot-tube pressure, with zero yaw at sweepback angles in the range 24 to 31 degrees. No explanation for this can yet be offered.

More experimental data on pressure recovery taken on similar designs of probe is available in a complementary R.A.E. Technical Report.<sup>5</sup>

## 8. Flow Direction Sensing

### 8.1. Pitch Sensing

The regular change of static pressure on the attachment line with change of sweepback angle, or change of attitude in pitch, has already been noted (Figs. 5 and 6). This suggested that the pressure in this region could be used as a flow direction sensor. More specifically, the pressure could be used to detect changes of flow direction in the plane of symmetry of the probe. A pressure tapping located anywhere along the leading edge of the compression surface could be used for this purpose. However, it has already been stated that the straight portion of the cylinder is not a necessary part of the probe and would in future be omitted. Therefore, a tapping on the curved portion must be used. The question arises as to what position on the curve should be chosen for the tapping. The limits of position are near to the leading tip or near to the pitot tube.

A theoretical prediction of the sensitivity of attachment line static pressure to change of sweepback angle on infinitely long cylinders is given in Appendix A. It is shown that at low subsonic values of free-stream Mach number the maximum sensitivity of static pressure to sweepback angle occurs at an angle of 45 degrees. The sweepback angle for maximum sensitivity falls with increasing Mach number reaching, for example, about 36.5 degrees at  $M_0 = 1.24$ . The available range of tapping locations allows the choice of local sweepback angle in the range from near 90 degrees at the tip to near 42 degrees by the pitot tube, with the probe at its 'design' sweepback angle of 35 degrees and with the pitot tube located in the position shown on Fig. 2a.

This probe is intended for use in supersonic flow, and therefore if the theory is used as a guide one would ideally choose a tapping located where the local sweepback is around 35 degrees. The closest tapping to this ideal position was the third back from the tip, that is the tapping closest to the pitot tube. This was located 39.1 mm from the tip, measured along the surface, where the local sweepback angle was about 50.8 degrees when  $\Lambda = 35$  degrees.

The measured variation with  $\Lambda$  of the pressure  $P_3$  at this location is shown on Fig. 11 for each test Mach number. There was some unsteadiness in  $P_3$  at the smaller values of sweepback when  $M_0 = 2.48$ . The sensitivities of pressure  $P_3$  to  $\Lambda$ , at  $\Lambda = 35$  degrees are given in non-dimensional form in Table 4.

### 8.2. Yaw Sensing

Static tappings were located symmetrically on either side of the attachment line in order to sense flow direction changes in yaw. The tappings were 36.6 mm downstream of the leading tip, disposed at 25 degrees on either side of the attachment line.

The difference between the pressures at these tappings is denoted by  $\Delta P_y$ . The variation of  $\Delta P_y/P_t$  with yaw angle is shown on Fig. 12, for the three test Mach numbers and with the probe swept back at an angle  $\Lambda$  of 35 degrees relative to the yawing support sting. The slopes of the curves on Fig. 12 at zero yaw are given in Table 5, together with the slopes

$$\frac{1}{q_0} \frac{d(\Delta P_y)}{d\beta}$$

## 9. Flow Deflection for Sonic Flow

The angle through which supersonic flow must be deflected in order to bring it locally to the sonic point is a function of

- (a) the geometry of the compression surface which is causing the deflection,
- (b) the free-stream Mach number, and,
- (c) gas properties.

The flow deflection which must be generated by the compression surface of this probe in air can be determined from Figs. 5 and 6. For example, at  $M = 1.53$  and  $\Lambda = 30$  degrees the sonic point is reached at a position 26.7 mm downstream of the tip. The flow has been turned approximately 31.7 degrees. Similarly at  $\Lambda = 40$  degrees the sonic point is 35.8 mm downstream of the tip giving a flow turning angle of 30.9 degrees. Hence in the region of the design sweepback, a flow deflection of about 31.3 degrees is required in air at  $M_0 = 1.53$ . Similarly at  $M_0 = 1.88$  and  $\Lambda = 35$  degrees the sonic point is reached when the flow has been deflected  $44\frac{1}{2}$  degrees. These two points are plotted on Fig. 13, where the theoretical deflection for sonic flow at the surfaces of several other types of compression surface is shown for comparison. The theories are exact solutions for the inviscid flow of a perfect gas with  $\gamma = 1.4$ .



The well-known wedge and cone compression surfaces need to deflect the flow relatively small amounts in comparison with the curved cylindrical compression surface of the probe. No theory exists as yet which can predict the sonic point on such a curved surface. However, in Appendix B an exact solution is presented for flow which is decelerated to the sonic point by a series of  $N$  long straight cylindrical compression surfaces. As a streamline in the plane of symmetry approaches the cylinders it follows a curved path which is similar in some respects to that of the streamline approaching the curved surface of the probe. The points plotted with diamond symbols on Fig. 13 show the limiting maximum Mach numbers for isentropic processes ahead of probes comprising  $N = 1, 2$  or  $3$  straight cylindrical compression surfaces. The broken line is the locus of these points. It can be seen that this theory over-estimates the turning required by the curved probe, and therefore a more applicable theory is required.

The best guidance on flow turning which can be given at present is from the two experimental points on Fig. 13. For example, rather a long extrapolation suggests that a turning of more than 60 degrees would be required to reach the sonic point from  $M_0 = 2.5$ , whereas the maximum turning angle available is 55 degrees with the curved probe when  $\Lambda = 35$  degrees. Therefore this particular geometry cannot be expected to produce a pressure recovery of unity at  $M_0 = 2.5$ .

A shorter extrapolation beyond the experimental points suggests that the available turning of 55 degrees might be expected to produce a pressure recovery of unity up to  $M_0 \approx 2.2$ .

## 10. Conclusions

(1) A probe comprising a pitot tube lying against a curved cylindrical compression surface has demonstrated a pressure recovery of 0.999 in air flowing at Mach numbers of 1.53 and 1.88.

(2) The pressure recovery is probably in the range 1.000 to 0.999 over the whole Mach number range up to 1.88.

(3) Measurements at Mach numbers 1.53 and 1.88 show that pressure recovery is substantially constant inside a flow misalignment plateau. The shape of the plateau is only partially known.

(4) There are indications that the probe should generate a pressure recovery close to unity at Mach numbers up to about 2.2.

(5) Work remains to be done in at least two areas:

(i) to determine the minimum practical size of the probe, and,

(ii) to extend upwards the range of Mach number over which it generates a high pressure recovery.

## Acknowledgments

I wish to express my thanks to Mr. A. R. G. Mundell of Aerodynamics Department, R.A.E., who carried out the experiments on this probe and to his Department for making available a supersonic wind tunnel.

## LIST OF SYMBOLS

$a$	Speed of sound
$F$	Multiplier converting pitot to stagnation pressure
$k$	$\sqrt{\frac{\gamma + 1}{2}}$
$M$	Mach number
$M_0$	Free-stream Mach number
$M_{0i}$	The maximum free-stream Mach number at which a probe can generate an isentropic compression
$n$	One of a series of long straight cylindrical compression surfaces
$N$	The number of compression surfaces in series employed by a probe
$P$	Static pressure
$P_t$	Stagnation (total) pressure
$P_3$	Static pressure at third tap from leading tip of probe
$P_\infty$	Free-stream static pressure
$\Delta P_y$	Pressure difference between tappings sensing yaw angle
$q_0$	Free-stream dynamic pressure, $q_0 = \frac{\gamma}{2} P_\infty M_0^2$
$R$	Pressure recovery
$T$	Thrust per unit area
$v$	Velocity
$x, y$	Co-ordinates of the leading edge profile and static tapping locations of the curved cylindrical compression surface
$\beta$	Yaw angle
$\gamma$	Ratio of specific heats
$\delta$	Flow deflection
$\delta_N$	Total flow deflection generated by $N$ surfaces in series
$\Lambda$	Sweepback angle of straight cylindrical (or the straight section of curved cylindrical) compression surface
$\Lambda'$	Theoretical sweepback of cylinder for the maximum sensitivity of $P_a$ to $\Lambda$
$\Lambda''$	Value of $\Lambda'$ for which $M_c = 1$
<i>Suffixes</i>	
$a$	Local value on attachment line
$c$	Cross-flow component
$n$	At attachment line of cylinder $n$

## REFERENCES

<i>No.</i>	<i>Author</i>	<i>Title, etc.</i>
1	A. A. Woodfield .. .. .	Thrust measurement in flight : The requirements, current situation and future possibilities. R.A.E. Technical Memorandum Aero 1175 (1969).
2	J. R. Baron .. .. .	Analytic design of a family of supersonic nozzles by the Friedrich's method. W.A.D.C. Technical Report 54-279, June 1954.
3	M. J. Goodyer .. .. .	A new stagnation pressure probe having a high pressure recovery in supersonic flow. Instrumentation in the Aerospace Industry, Vol. 18 (1972). Instrument Society of America, Pittsburgh.
4	J. A. F. Hill, <i>et al</i> .. .. .	Mach number measurements in high speed wind tunnels. AGARDograph 22, October 1956.
5	A. R. G. Mundell .. .. .	Tests on probes designed to measure stagnation pressure directly in a supersonic stream. A.R.C. R. & M. 3755 (1973).

## APPENDIX A

### The Variation of Attachment Line Static Pressure with Sweepback Angle and Mach Number

In an earlier paper<sup>3</sup> an exact theory is developed for the static pressure on the attachment line of an infinitely long swept straight cylinder. The static pressure is equal to the total pressure of the crossflow component of velocity when the crossflow component of the free-stream Mach number is unity or less, and is given by

$$P_a = P_\infty \left[ 1 + \frac{\gamma - 1}{2} M_0^2 \cos^2 \Lambda \right]^{\gamma/(\gamma-1)} \quad (\text{A-1})$$

When the crossflow is supersonic the static pressure  $P_a$  given by the above equation must be reduced. This is to account for a shock parallel to the cylinder which the streamlines must penetrate as they approach the attachment line.

The rate of change of static pressure on the attachment line with sweepback angle,  $dP_a/d\Lambda$  from equation (A-1) is

$$\begin{aligned} \frac{dP_a}{d\Lambda} &= -\frac{\gamma}{2} P_\infty M_0^2 \sin 2\Lambda \left[ 1 + \frac{\gamma - 1}{2} M_0^2 \cos^2 \Lambda \right]^{1/(\gamma-1)} \\ &= -q_0 \sin 2\Lambda \left[ 1 + \frac{\gamma - 1}{2} M_0^2 \cos^2 \Lambda \right]^{1/(\gamma-1)} \end{aligned} \quad (\text{A-2})$$

where the free-stream dynamic head is given by

$$q_0 = \frac{\gamma}{2} P_\infty M_0^2.$$

At low values of  $M_0$  it is convenient to express  $dP_a/d\Lambda$  in terms of the dynamic head, in which case equation (A-2) becomes simply

$$\frac{dP_a}{d\Lambda} \frac{1}{q_0} = -\sin 2\Lambda. \quad (\text{A-3})$$

The sensitivity of  $P_a$  to  $\Lambda$  therefore is a maximum at a sweepback angle of 45 degrees at low airspeeds, when the change of pressure is just  $q_0$  per radian. At higher Mach numbers the optimum sweepback angle (that giving a maximum pressure sensitivity of  $P_a$  to  $\Lambda$ ) is not 45 degrees but may be obtained by differentiating equation (A-2) and equating to zero, the resultant angles being valid provided that  $M_0 \cos \Lambda \leq 1$ . The relation between  $M_0$  and the optimum angle  $\Lambda'$  is then

$$M_0^2 = \frac{1 - \tan^2 \Lambda'}{\sin^2 \Lambda' - \frac{\gamma - 1}{2} (\cos^2 \Lambda' - \sin^2 \Lambda')} \quad (\text{A-4})$$

The value of  $\Lambda'$  for which the crossflow component of free-stream Mach number is unity ( $M_0 \cos \Lambda' = 1.0$ ), marks the upper Mach number limit of validity of equation (A-4). If the corresponding value of the sweepback angle is  $\Lambda''$ , then from equation (A-4)

$$\tan^2 \Lambda'' = \frac{\gamma + 1}{\gamma + 3}. \quad (\text{A-5})$$

For  $\gamma = 1.4$ ,  $\tan^2 \Lambda'' = 0.545454 \dots$  and  $\Lambda'' \approx 36.45$  degrees. The corresponding free-stream Mach number is 1.2432. The variation of  $dP_a/d\Lambda \times 1/q_0$  with  $M_0$  at the optimum sweepback angle  $\Lambda'$  from equation (A-4) is shown on Fig. 14 for the Mach number range 0 to 1.2432. The variation of  $\Lambda'$  with  $M_0$  is also shown. The remaining information on this figure is presented for  $\Lambda = 35$  degrees, the design sweepback angle of the straight section of the probe. For this angle the theoretical sensitivities are expressed as  $(1/q_0)(dP_a/d\Lambda)$  which is a convenient form for use at low  $M_0$ , and as  $(1/P_\infty)(dP_a/d\Lambda)$  which may be a more convenient form for use at higher Mach numbers.

The variation of  $P_a$  with  $\Lambda$  has been measured along the length of the compression surface at  $M_0 = 1.53$  and  $1.88$ . The data are given on Figs. 5 and 6. The sensitivity of  $P_a$  to  $\Lambda$ , referred to stagnation pressure  $P_t$ , at a position on the straight section of the compression surface  $87.1$  mm from the leading tip and at the design sweepback angle of  $35$  degrees, is also shown on Fig. 14.

There is fair agreement between theory and experiment. In view of this it may be reasonable to be guided by this theory in the design of probes. A particular conclusion relevant to flow direction sensing is that the best sensitivity in the low supersonic range is obtained at sweepback angles close to but less than  $45$  degrees.

## APPENDIX B

### Mach Number and Flow Deflection Relationships for a Series Arrangement of 'Infinite' Swept Straight Compression Surfaces

The theoretical behaviour of the flow in the plane of symmetry of a hypothetical infinitely long straight compression surface, swept relative to the free stream, is available.<sup>3</sup> The highest free-stream Mach number at which a pitot tube mounted on the attachment line facing into the local flow will register full free-stream stagnation pressure occurs when both the local Mach number at the pitot tube and the component of free-stream Mach number directed at right angles to the axis of the compression surface are unity. For  $\gamma = 1.4$  this condition is reached at a free-stream Mach number of  $(2.2)^{\frac{1}{2}} \approx 1.483$  and with a sweepback of the compression surface of 47.61 degrees. The streamline which is sampled by the pitot tube is deflected through 42.39 degrees during its deceleration from  $M_0 = 1.483$  in the free stream to  $M = 1$  on the attachment line. No further deflection occurs during the subsequent deceleration of that streamline to  $M = 0$  at the opening of the pitot tube.

In the region of the flow field immediately adjacent to the attachment line of this type of compression surface, the flow is uniform and parallel to the attachment line. It is conceivably possible to mount a second geometrically similar but much smaller compression surface in such a region of uniform flow. It is then possible to postulate a deceleration of the free stream to sonic point conditions in two distinct stages. The first deceleration would be generated by a large-dimensioned compression surface arranged at a sweepback angle such that the crossflow component of Mach number is just sonic in order to avoid the formation of a bow shock. The streamline which is to be sampled by the pitot tube is then deflected until it runs parallel to the axis of this compression surface and adjacent to its attachment line. In this region the streamline comes under the influence of the second, much smaller straight compression surface which is again arranged so that the Mach number component of the local flow directed across its axis is just unity. The pitot tube would lie against the attachment line of the smaller compression surface. For the special case where the local Mach number of the sampled streamline is just unity as it approaches the pitot tube, the combination of two compression surfaces with pitot tube forms a probe which is operating at a limiting maximum Mach number for entirely isentropic processes along the path of the streamline. It will be shown later that the pitot tube would register full free-stream stagnation pressure at a free-stream Mach number of 1.91.

A probe which operates according to the above notions is impractical because of the requirement for compression surfaces which at least extend infinitely far in the generally upstream direction. However, it has been shown<sup>3</sup> that in the case of single cylindrical compression surfaces a probe of finite size can be devised which behaves in a manner close to that predicted by these simple theories. Therefore conceivably two finite sized surfaces as described above sharing in series the function of decelerating the sampled streamline would also behave close to theory. This is some justification for a theoretical pursuit of the notion with the object of determining total flow deflections and limiting Mach numbers for isentropic compression for this type of probe.

The notion of 'staging' the deceleration process of the streamline can be extended in the manner described above to a consideration of  $N$  surfaces. For a probe comprising  $N$  compression surfaces, each straight and infinitely long and lying one within the attachment-line flow field of another, the last compression surface encountered by the sampled streamline would carry the pitot tube on its attachment line. For the free-stream Mach number to be a maximum limit for there to be isentropic compression processes everywhere along the streamline, the local Mach number on this last encountered attachment line would be unity. A theory for such a probe will now be developed.

The set of  $N$  compression surfaces is numbered against the flow. Hence, number 1 is that carrying the pitot tube, while  $N$  is the largest and that which first influences the sampled streamline. Consider the  $n$ th surface, where  $N > n > 1$ . This surface lies entirely within the attachment line flow field of the  $(n + 1)$ th surface, where the velocity is uniformly  $v_{n+1}$ , Mach number  $M_{n+1}$  and speed of sound  $a_{n+1}$ . A sketch of the geometrical arrangement of surface  $n$  adjacent to the attachment line of surface  $n + 1$  is shown on Fig. 15. The sweepback angle of surface  $n$  is so arranged that the component of  $M_{n+1}$  which is directed at right angles to its axis is unity. The corresponding velocity component is therefore  $a_{n+1}$ . The formation of a bow shock ahead of surface  $n$  is thereby avoided, a condition which is maintained by all surfaces.

Velocity component  $a_{n+1}$  is destroyed as the streamline converges onto the attachment line of surface  $n$ , whereas the velocity component parallel to the axis of surface  $n$ ,  $v_n$ , will remain constant.

The latter statement is true provided that there is no obstruction to the flow on the attachment line of  $n$ . While all surfaces from  $n - 1$  to 1 lie in this region, it is assumed that they are so small that their presence does not invalidate the last statement in the preceding paragraph. The velocity triangle on Fig. 15 is constructed

assuming that the component of  $v_{n+1}$  directed at right angles to surface  $n$  is just  $a_{n+1}$ . As component  $a_{n+1}$  is destroyed the static temperature of the gas is increased by factor  $(\gamma + 1)/2$ , hence  $a_n = ka_{n+1}$  where  $k^2 = (\gamma + 1)/2$ . Similarly,  $M_n = v_n/a_n = v_n/ka_{n+1}$  and  $\delta_n = \sin^{-1} 1/M_{n+1}$ .

From the velocity triangle,

$$(v_{n+1})^2 = v_n^2 + (a_{n+1})^2$$

hence  $(M_{n+1})^2 = 1 + k^2 M_n^2$ .

The limiting maximum free-stream Mach number for isentropic flow along the sampled streamline is  $M_{0l}$ . At this value of free-stream Mach number the Mach number of the crossflow component of the flow field ahead of each compression surface is just unity, as is the Mach number on the attachment line of the last encountered surface. For the case of  $N$  surfaces in series,

$$(M_{0l})^2 = 1 + k^2 + k^4 + \dots + k^{2N}.$$

The variation of  $M_{0l}$  with  $N$ , together with the total flow deflection  $\delta_N$  generated by  $N$  surfaces, are given in table B1.

TABLE B1  
 $M_{0l}$  and  $\delta_N$  for  $N$  straight cylindrical surfaces in series ( $\gamma = 1.4$ )

$N$	1	2	3	5	10	15	20
$M_{0l}$	1.483	1.908	2.317	3.151	5.67	9.35	15.00
$\delta_N$ (degrees)	42.39	74.00	99.57	139.58	204.13	241.91	265.18

$\delta_N$  points for  $N = 1, 2, 3$  are plotted on Fig. 13.

TABLE 1  
Measured and Calculated Leading-Edge Static Pressures

(a) $M_0 = 1.53$			(b) $M_0 = 1.88$		
$\Lambda$ degrees	$P_a/P_t$		$\Lambda$ degrees	$P_a/P_t$	
	Measured	Theory		Measured	Theory
10	0.904	0.897	20	0.709	0.695
20	0.857	0.830	25	0.671	0.653
30	0.780	0.725	30	0.630	0.603
40	0.673	0.607	35	0.579	0.549
47.2	0.590	0.517	40	0.530	0.491
			45	0.474	0.432
			50	0.420	0.374

TABLE 2  
Ranges of Sweepback where  $1.000 > R \geq 0.998$  at Zero Yaw

$M_0 = 1.53$		$M_0 = 1.88$	
Limits on $\Lambda$ , degrees	Total sweepback range, degrees	Limits on $\Lambda$ , degrees	Total sweepback range, degrees
$22\frac{1}{2}$ to $47\frac{1}{2}$	25	26 to 42	16

TABLE 3  
Ranges of Yaw where  $1.000 > R \geq 0.998$  at Constant Sweepback  $\Lambda = 35^\circ$

$M_0 = 1.53$		$M_0 = 1.88$	
Limits on yaw, degrees	Total yaw range, degrees	Limits on yaw, degrees	Total yaw range, degrees
$-7\frac{1}{2}$ to +10	$17\frac{1}{2}$	-11 to +12	23



TABLE 4  
Sensitivity of Static Pressure  $P_3$  to  $\Lambda$ , at  $\Lambda = 35^\circ$

$M_0$	1.53	1.88	2.48
$\frac{1}{P_t} \frac{dP_3}{d\Lambda}$ per degree	0.0119	0.0117	0.0096
$\frac{1}{P_t} \frac{dP_3}{d\Lambda}$ per radian	0.682	0.669	0.550
$\frac{1}{q_0} \frac{dP_3}{d\Lambda}$ per degree	0.0278	0.0306	0.0369
$\frac{1}{q_0} \frac{dP_3}{d\Lambda}$ per radian	1.595	1.756	2.116

TABLE 5  
Yaw Sensitivities at  $\Lambda = 35^\circ$

$M_0$	1.53	1.88	2.48
$\frac{1}{P_t} \frac{d(\Delta P_y)}{d\beta}$ per degree	0.0170	0.0141	0.0087
$\frac{1}{P_t} \frac{d(\Delta P_y)}{d\beta}$ per radian	0.974	0.808	0.500
$\frac{1}{q_0} \frac{d(\Delta P_y)}{d\beta}$ per degree	0.0398	0.0370	0.0335
$\frac{1}{q_0} \frac{d(\Delta P_y)}{d\beta}$ per radian	2.28	2.12	1.92

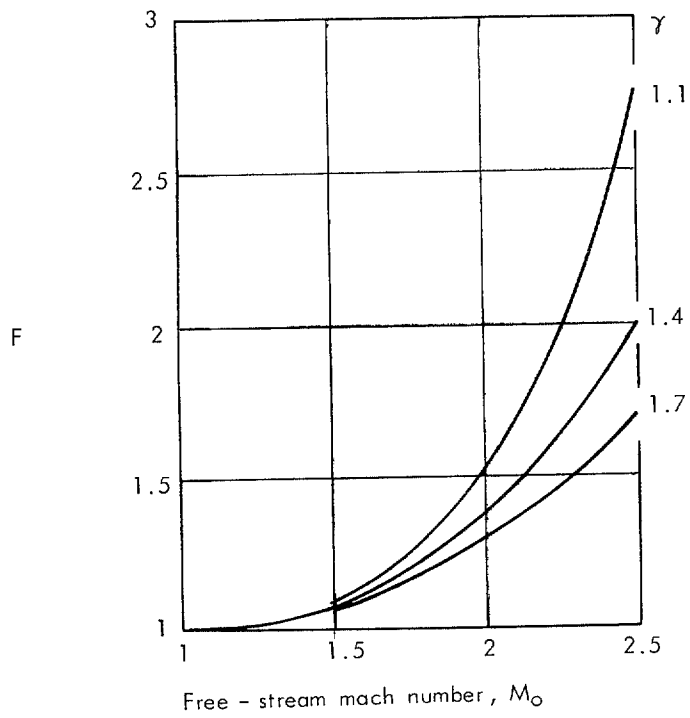
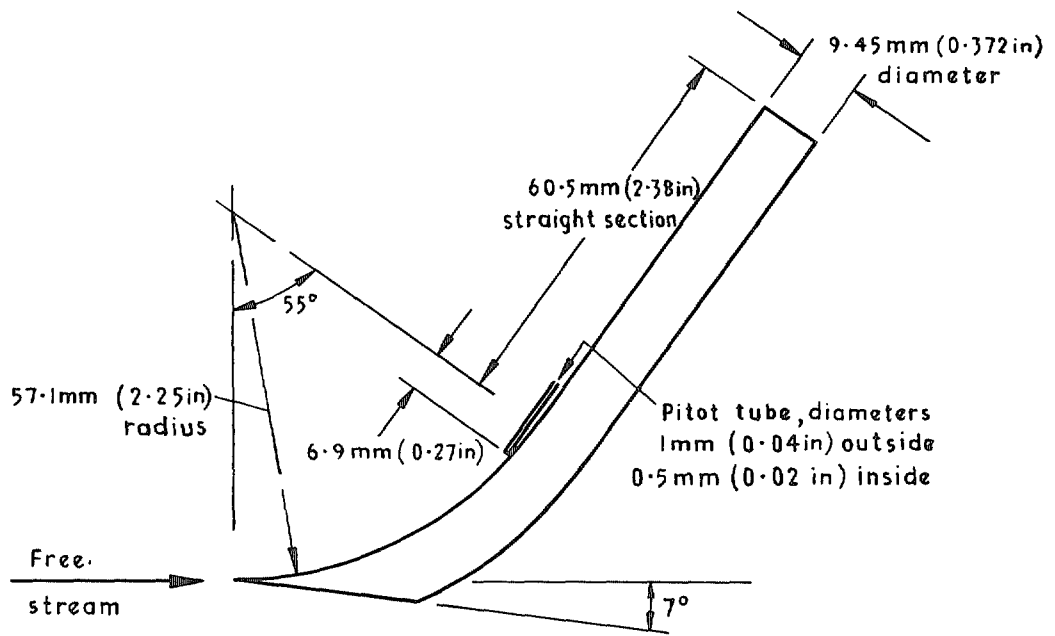
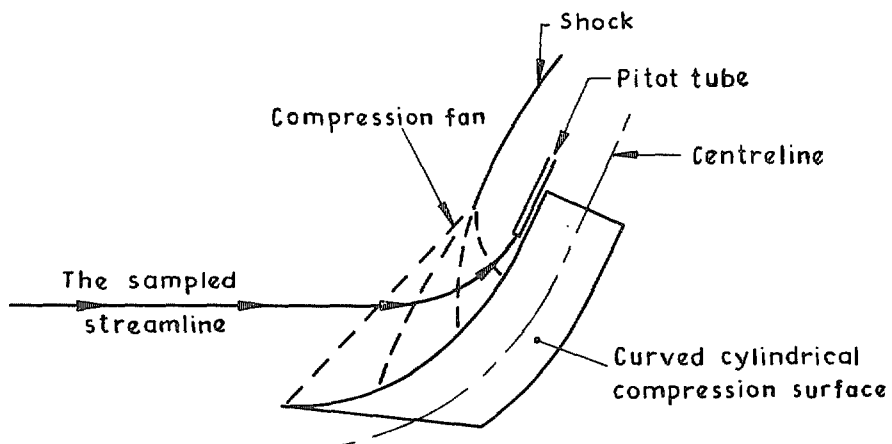


FIG. 1. The factor  $F$  converting pitot pressure into stagnation pressure.

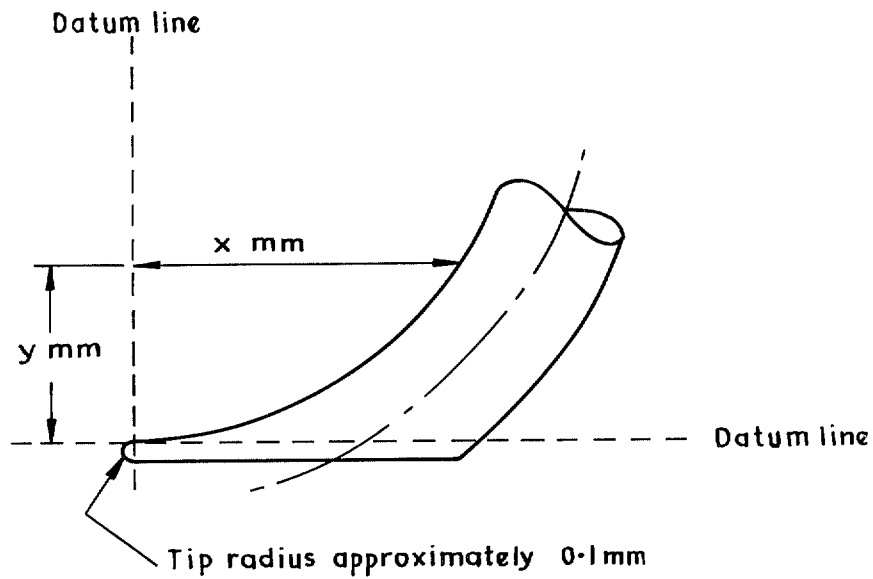


a Nominal dimensions of the probe



b A sketch of the flow field ahead of the compression surface

FIG. 2a & b. Drawings of the probe.



x	y	x	y
0.	0.	34.508	17.148
2.159	.399	37.300	20.363
5.527	.922	39.187	22.664
9.578	1.908	41.156	25.621
13.432	3.165	43.017	28.390
17.935	5.044	44.674	30.876
22.799	7.506	47.435	35.286
27.376	10.701	50.122	40.002
30.620	13.381	52.304	43.746
32.578	15.189	54.823	48.247

#### Static pressure tapping locations

Tap No	x	y
1	14.592	3.597
2	25.872	9.644
3	33.696	16.309
4	40.305	24.331

FIG. 3. Measured co-ordinates of compression surface.

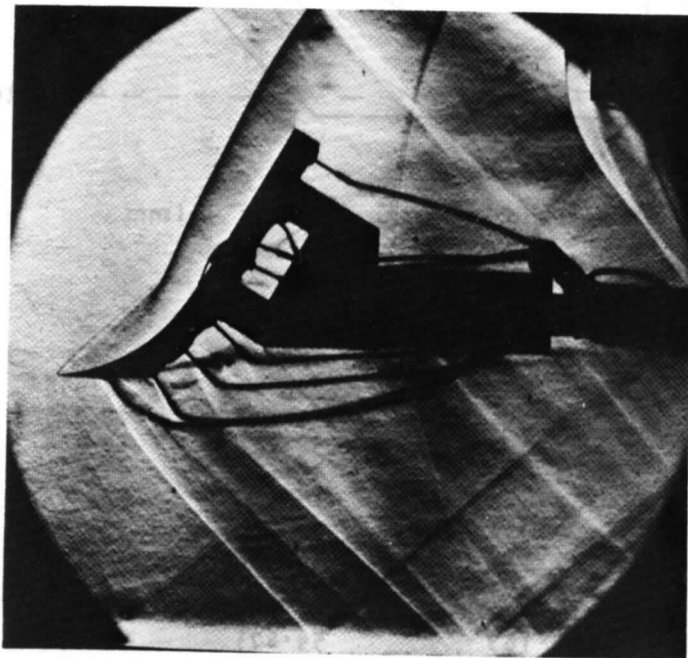


FIG. 4. A schlieren picture of the flow around the probe at  $M_0 = 1.53$ .

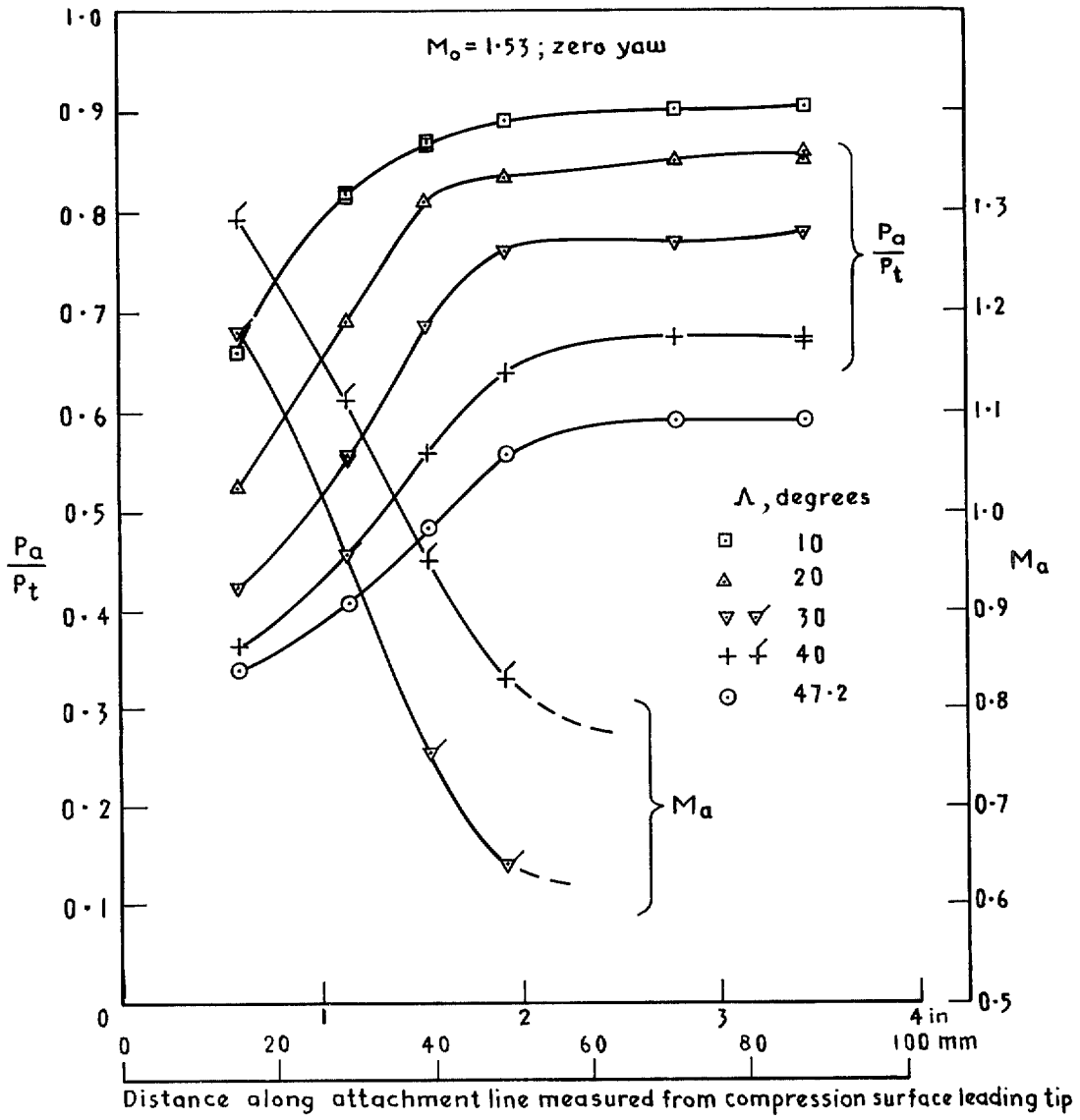


FIG. 5. The distribution of static pressure  $P_a$  and local Mach number  $M_a$  along the attachment line.  $M_0 = 1.53$ .

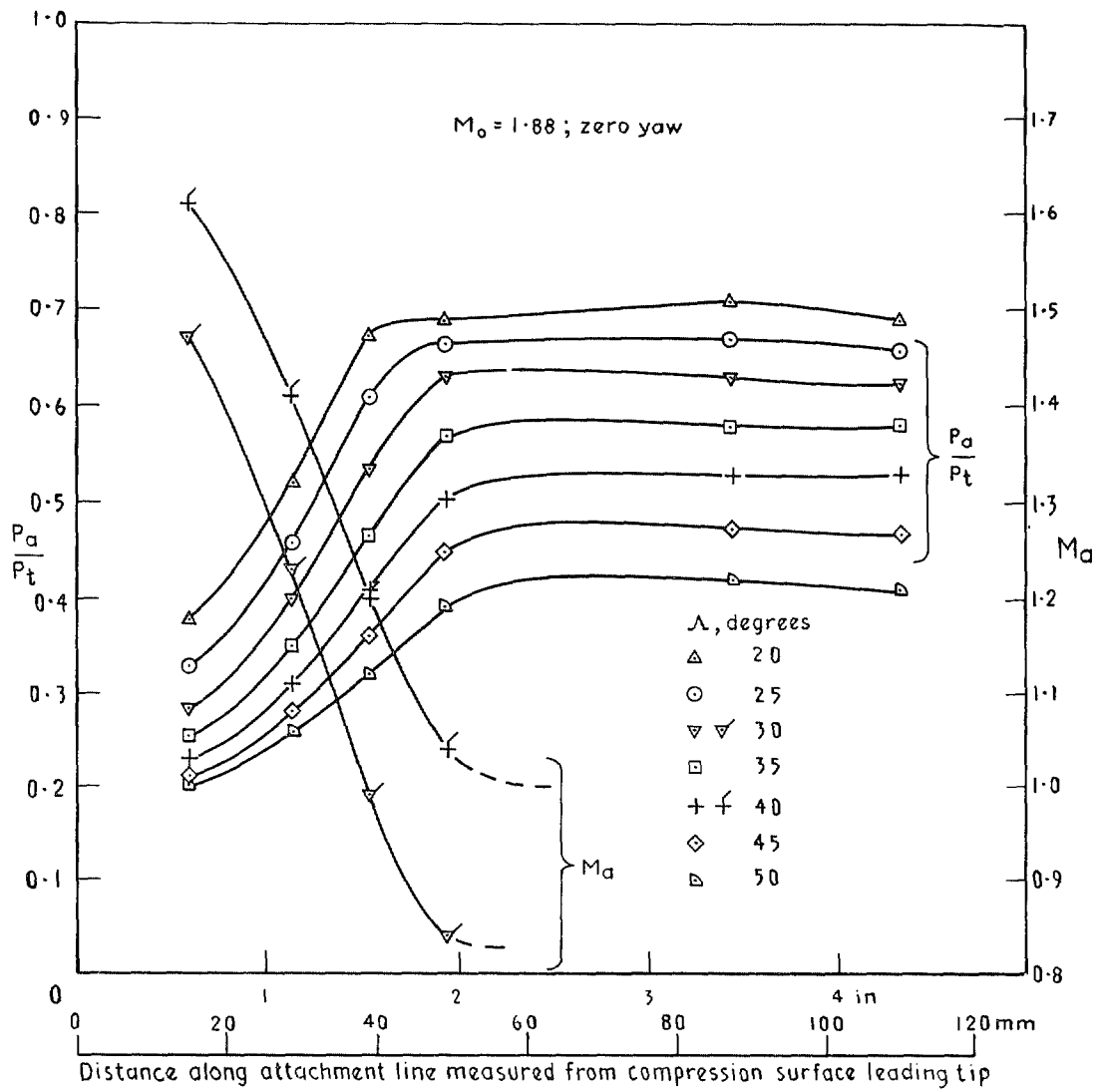


FIG. 6. The distribution of static pressure  $P_a$  and local Mach number  $M_a$  along the attachment line,  $M_0 = 1.88$ .

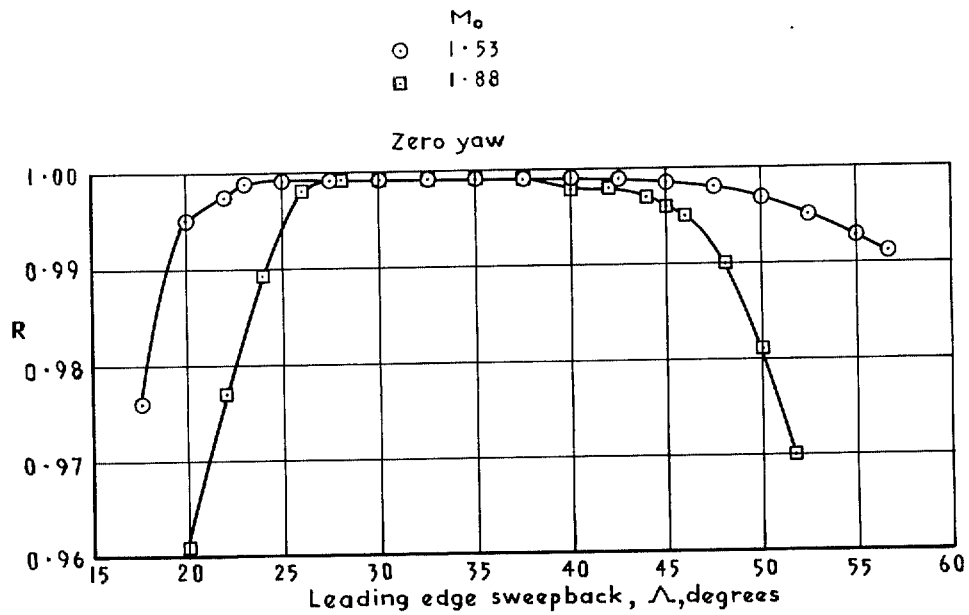


FIG. 7. The variation of pressure recovery  $R$  with sweepback  $\Lambda$  at zero yaw, and at free-stream Mach numbers  $M_0$  of 1.53 and 1.88.

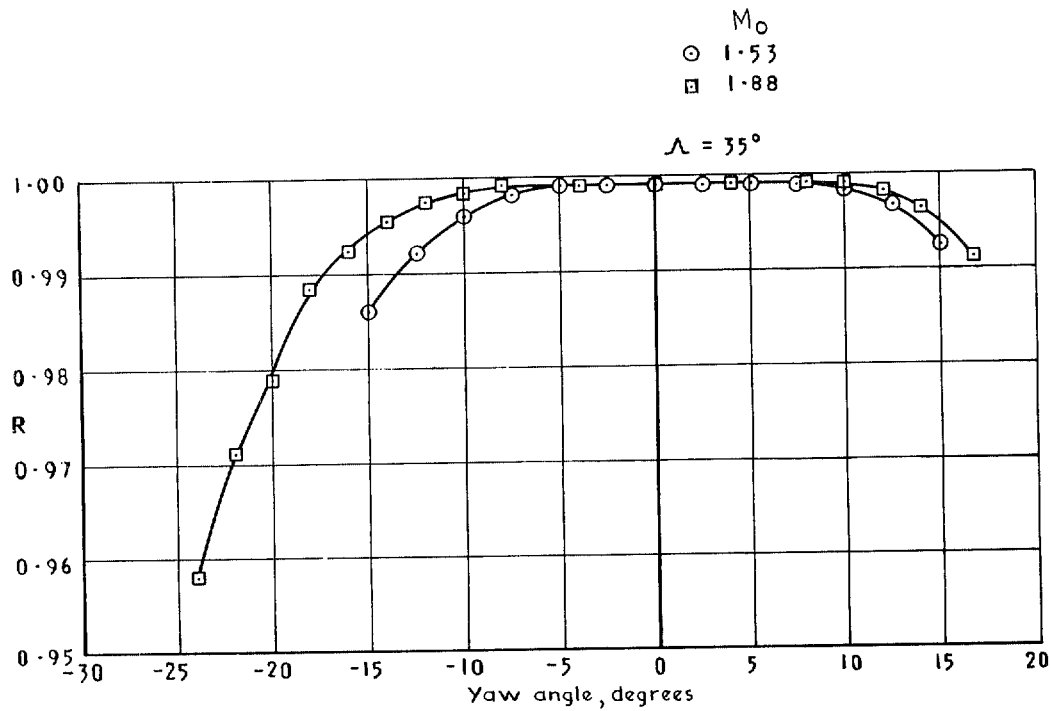


FIG. 8. The variation of pressure recovery  $R$  with yaw, at constant sweepback  $\Lambda$  and free-stream Mach numbers  $M_0$  of 1.53 and 1.88.



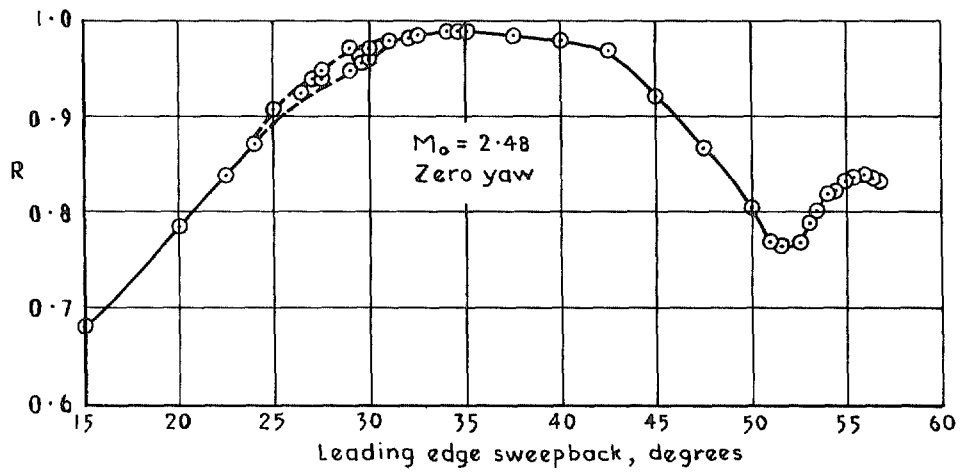


FIG. 9. The variation of pressure recovery  $R$  with sweepback  $\Lambda$  at zero yaw, and a free-stream Mach number 2.48.

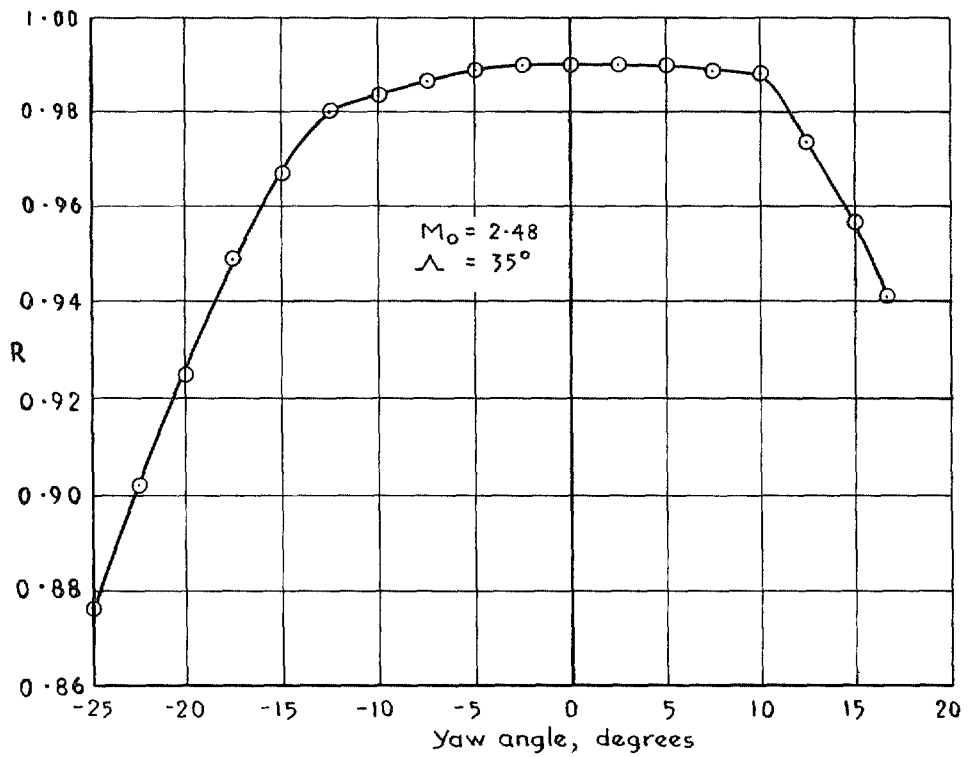


FIG. 10. The variation of pressure recovery  $R$  with yaw, at constant sweepback  $\Lambda$  and a free-stream Mach number  $M_0$  of 2.48.

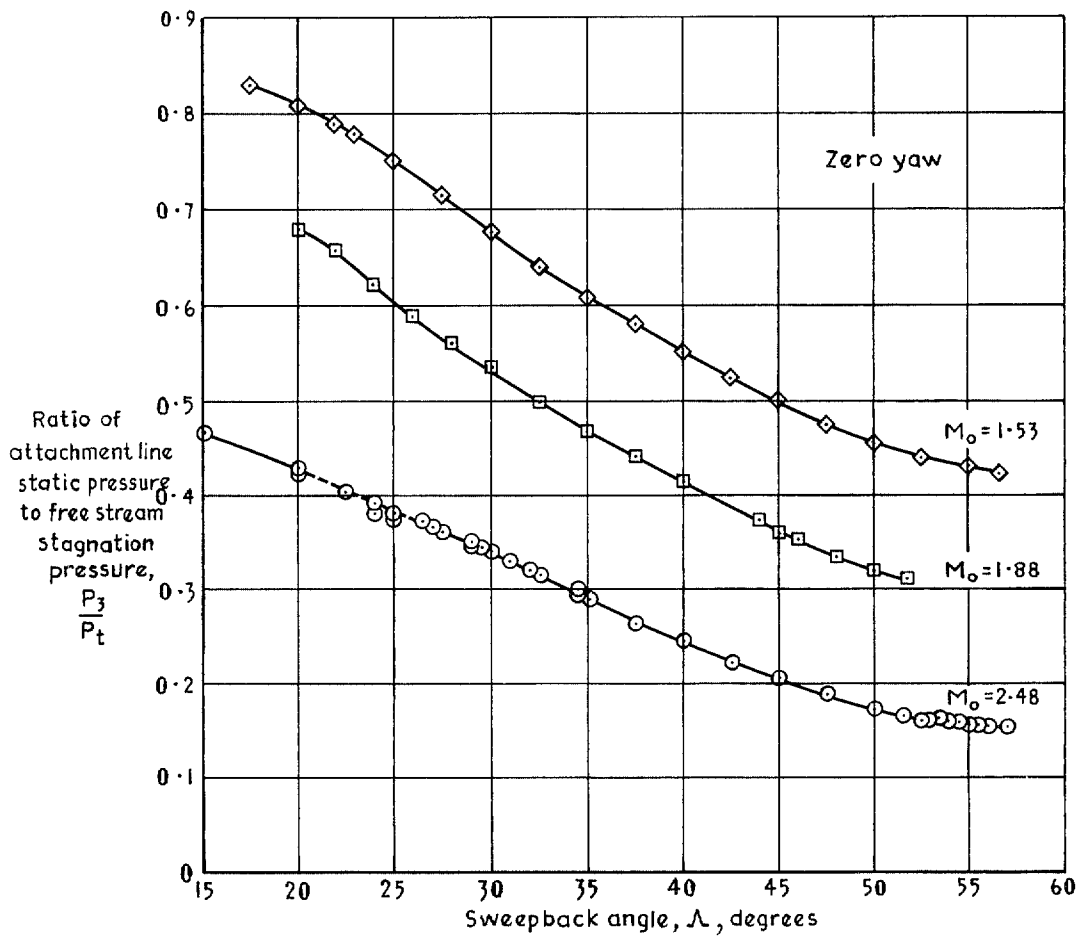


FIG. 11. The variation of static pressure with sweepback angle  $\Lambda$  and free-stream Mach number  $M_0$  for one station on the attachment line of the curved compression surface, 39.1 mm (1.54 in.) from the leading tip.

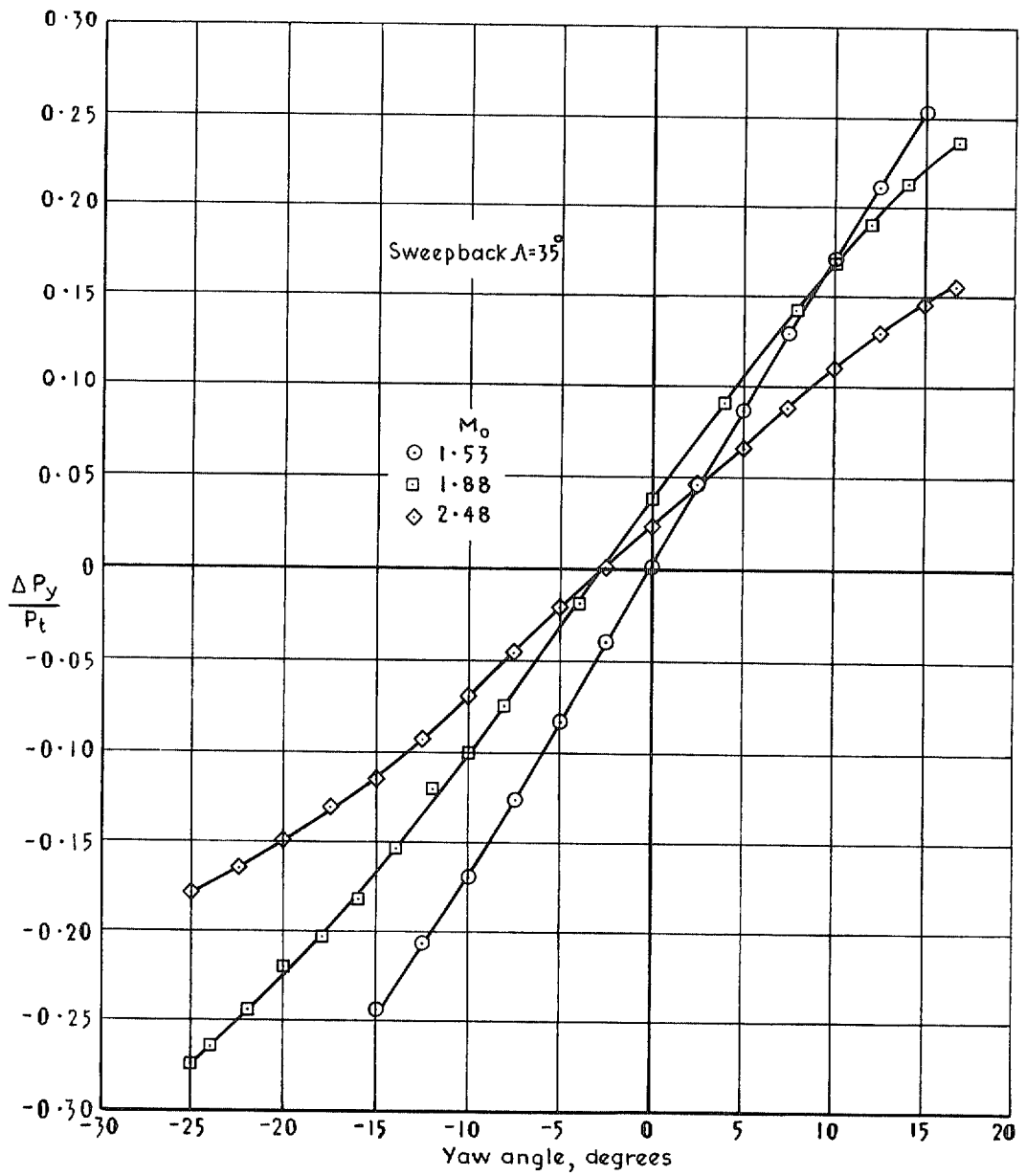


FIG. 12. Calibrations of compression surface tappings for sensing yaw angle.

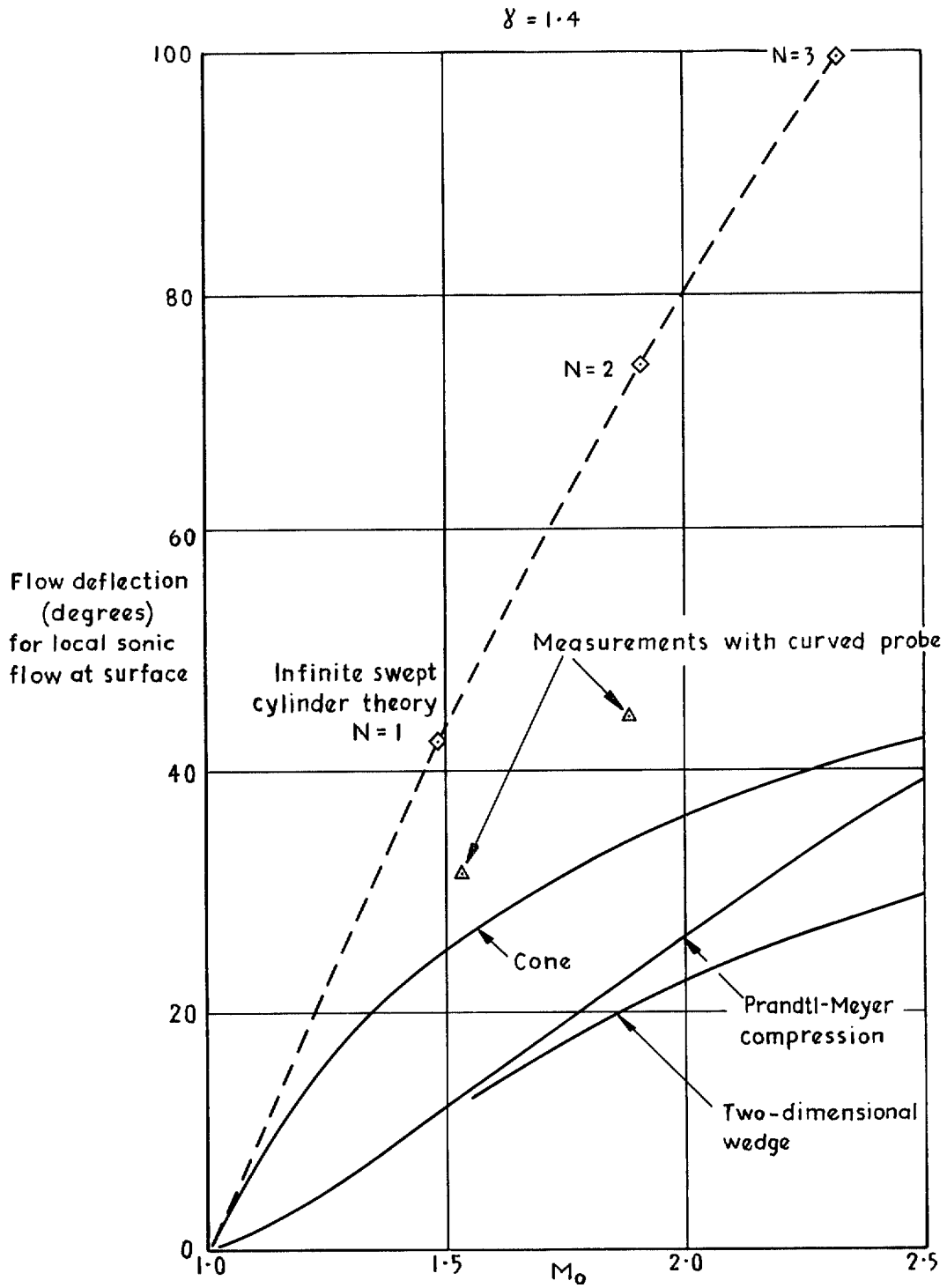


FIG. 13. Flow deflection required by different compression surfaces to generate locally sonic flow at the surface.

Key : — Exact theory for infinite swept cylinders  
 ⊙ Measurements of  $\frac{1}{P_t} \frac{dP_a}{d\Lambda}$  on the straight section of the probe shown on Fig.2 at 87.1mm (3.43 in) from the leading tip

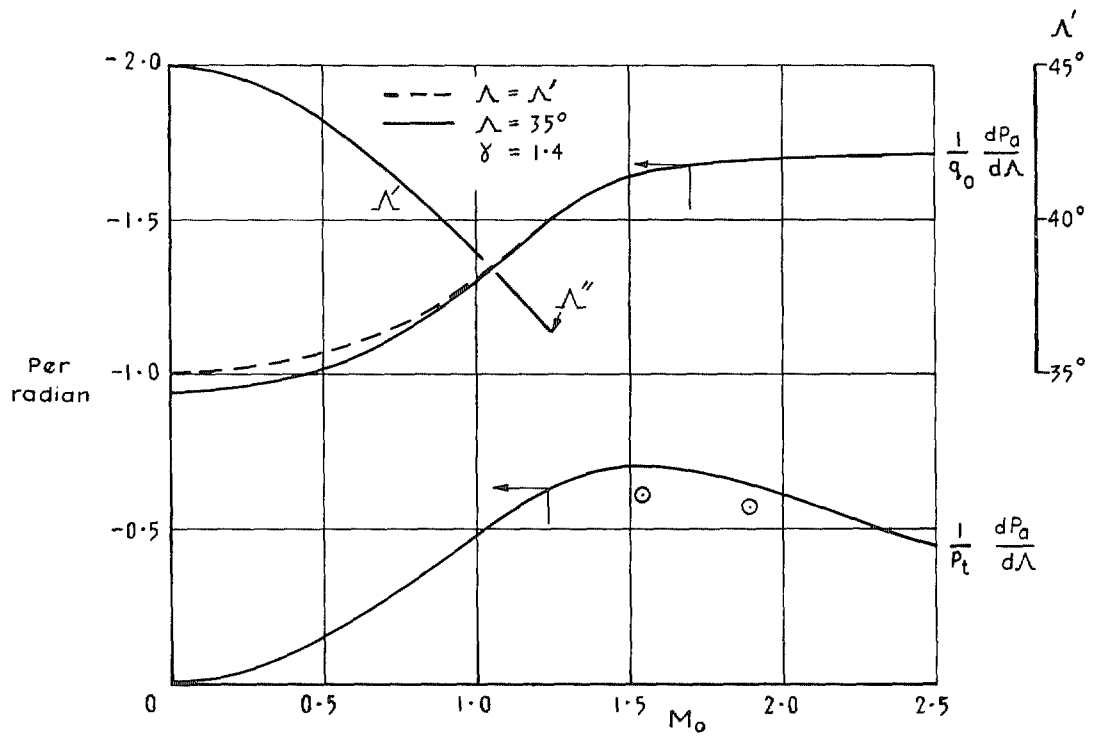


FIG. 14. The sensitivity of leading edge static pressure  $P_a$  to change of sweepback angle.

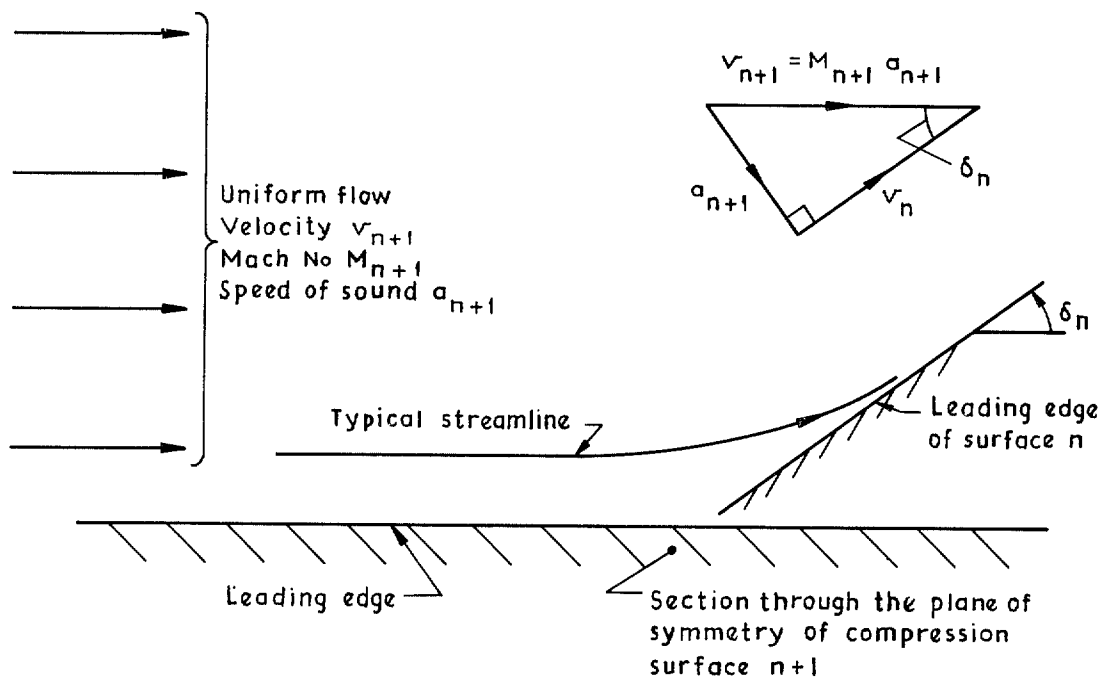


FIG. 15. The geometrical arrangement of compression surface  $n$  in the leading edge flow field of surface  $n + 1$ .

© Crown copyright 1975

HER MAJESTY'S STATIONERY OFFICE

*Government Bookshops*

49 High Holborn, London WC1V 6HB  
13a Castle Street, Edinburgh EH2 3AR  
41 The Hayes, Cardiff CF1 1JW  
Brazennose Street, Manchester M60 8AS  
Southey House, Wine Street, Bristol BS1 2BQ  
258 Broad Street, Birmingham B1 2HE  
80 Chichester Street, Belfast BT1 4JY

*Government publications are also available  
through booksellers*